

Article

Sandstone Porosity Evolution and Reservoir Formation Models of the Paleogene Huagang Formation in Yuquan Structure of West Lake Sag, East China Sea Basin

Yonghuang Cai ^{1,†}, Zhengxiang Lv ^{1,2,*}, Yuanhua Qing ^{3,†}, Cheng Xie ¹, Bingjie Cheng ¹, Zheyuan Liao ¹ and Bing Xu ¹

¹ College of Energy Resources, Chengdu University of Technology, Chengdu 610059, China; 2023050136@stu.cdut.edu.cn (Y.C.); xiecheng@stu.cdut.edu.cn (C.X.); 2023050144@stu.cdut.edu.cn (B.C.); liaozheyuan@stu.cdut.edu.cn (Z.L.); xubing@stu.cdut.edu.cn (B.X.)

² State Key Laboratory of Oil and Gas Reservoir Geology and Exploitation, Chengdu University of Technology, Chengdu 610059, China

³ School of History and Geography, Chengdu Normal University, Chengdu 611130, China; 051061@cdnu.edu.cn

* Correspondence: lvzhengxiang13@cdut.edu.cn

† Co-first author.

Abstract: The West Lake Sag is abundant in oil and gas reserves, primarily in the Huagang Formation reservoir which serves as the primary source of production. The level of exploration is rather high, but there are still some unresolved issues, such as an unclear understanding of pore evolution features and reservoir growth mode. To tackle the aforementioned problems, this study employs optical microscopic examination, scanning electron microscope analysis, inclusion analysis, isotope analysis, X-ray diffraction analysis, and other techniques to elucidate the primary factors governing reservoir development and establish an analytical model regarding the cause of the sandstone reservoir. The results are as follows: (1) The sandstone reservoirs of the Huagang Formation of the Yuquan (abbreviated to YQ) Structure are now in the mesomorphic A stage as a whole, and minerals such as 4-phase authigenic quartz, 2-phase illite, 2-phase chlorite, 1-phase kaolinite, 1-phase ammonite mixing layer and 2-phase carbonate were formed during the diagenesis. (2) Feldspar and carbonate solution pores make up the majority of the reservoir space. About 10% of the porosity is made up of carbonate solution pores, which are the most prevalent reservoir space. Carbonate solution pores are primarily made up of metasomatic carbonate solution pores and cemented carbonate solution pores. Feldspar solution pores come next, contributing roughly 6.2% of the porosity. At 1.8%, residual intergranular holes are the least common. (3) The four main processes listed below are responsible for the creation of pores in the sandstone of the Huagang creation. The early carbonate cements resist the destruction of mechanical compaction and effectively preserve intergranular volume. The high content of feldspar provided a material basis for later dissolution. Early chlorite surrounding the edges of particles reduced the damage of authigenic minerals to porosity. The faults and cracks formed by the later structural inversion connected to the acidic water in the atmosphere, causing the dissolution of carbonate minerals and feldspar in the sandstone of the Huagang Formation. (4) Carbonate dissolution + feldspar dissolution type, carbonate dissolution type, and feldspar dissolution type are the three main types of reservoir formation in the Huagang Formation; the first two types mainly develop in the Upper Huagang Formation, while the latter mainly develops in the lower part of the Huagang Formation. The research results are conducive to the establishment of a geological prediction model for high-quality reservoirs of different geneses in the Huagang Formation and promote the exploration process of deep-seated hydrocarbons in the West Lake Sag.

Keywords: East China Sea basin; West Lake Sag; Yuquan Structure; Huagang Formation; porosity evolution; reservoir formation model



Citation: Cai, Y.; Lv, Z.; Qing, Y.; Xie, C.; Cheng, B.; Liao, Z.; Xu, B. Sandstone Porosity Evolution and Reservoir Formation Models of the Paleogene Huagang Formation in Yuquan Structure of West Lake Sag, East China Sea Basin. *Minerals* **2024**, *14*, 899. <https://doi.org/10.3390/min14090899>

Academic Editors: Tivadar M. Tóth and Yubin Bai

Received: 24 May 2024

Revised: 20 August 2024

Accepted: 27 August 2024

Published: 31 August 2024



Copyright: © 2024 by the authors. Licensee MDPI, Basel, Switzerland. This article is an open access article distributed under the terms and conditions of the Creative Commons Attribution (CC BY) license (<https://creativecommons.org/licenses/by/4.0/>).

1. Introduction

Porosity, as the main location for underground oil and gas resources, has a significant impact on hydrocarbon migration and enrichment, which determines the direction of searching for high-quality reservoirs and always acts as a crucial geological indicator for effective exploitation [1–3]. The West Lake Sag is the largest and richest hydrocarbon area on the East China Sea continental shelf [4]. Depths of exploration layers in the West Lake Sag reach intermediate to deep [5], and low-permeability tight reservoirs are becoming the main exploration objects. More than 100 billion cubic meters of hydrocarbon reserves have been discovered in well A area in which the Oligocene Huagang Formation is the major hydrocarbon bearing interval [6,7].

Around the world, there are several locations where sandstone reserves in reverse tectonic zones are being drilled for oil and gas [8–12]. The timing and development of reverse structures are crucial, as they directly influence reservoir formation and hydrocarbon accumulation [13,14]. Mature oil and gas production has been reached in the Watch and Green River Formations of the Uinta Basin due to reverse tectonic action in the North American Rocky Mountains region [10]. The Po and Valais basins in the western Alps of Europe have sandstone reservoirs in a reverse tectonic setting [11]. Stratigraphic folds are formed in the Songliao Basin of China as a result of reverse tectonic activity, which are crucial in the formation of vertically layered oil reservoirs that have anticlinal features [12]. The deep water area of the Qiongdongnan Basin—Songnan Baodao Depression, has formed a large anticline trap in the reverse structural zone [13]. The development of the Yuquan structural fault within the West Lake Sag can be divided into three stages [14]. Significantly, periods of tectonic compression have shown a strong association with the formation of oil and gas, so the Yuquan Structure can be identified as a highly suitable area for exploration [14]. This relation highlights the importance of structural tectonics in regulating hydrocarbon accumulation [14].

The Huagang Formation can be divided into upper and lower sub-segments, and there are five sandstone groups including H1 to H5 from top to bottom in the upper sub-segment and seven sandstone groups like H6 to H12 in the lower sub-segment [4]. Several findings indicate that the reservoir of the Huagang Formation is predominantly composed of fine to medium terrigenous clasts with low matrix and kaolinite, which has poor reservoir quality; that reservoir spaces are dominated by primary and secondary pores [15]; and that burial compaction is responsible for generally tight and low permeability [16]. Chlorite rims and dissolution are the key constructive diagenesis processes. For example, sand groups of H3 and H4 with well-developed chlorite rims have more dissolution porosities than sand groups of H5 and H6 with poorly developed chlorite rims [17].

Previous studies lack detailed analysis on the types, proportions, and vertical variation of secondary pores of different origins and the impact of retentive diagenesis on reservoir development, which limits accurate understandings of reservoir types and formation mechanisms [11], prevents the establishing geological of prediction models for high-quality reservoirs of different origins, and restrict exploration progression of deep oil and gas in West Lake Sag.

A combination of quantitative and qualitative approaches was used in this study. Through thin sections (obtaining characteristics of rock and mineral, authigenic mineral characteristics, reservoir space characteristics, etc.), scanning electron microscopy analysis, fluid-inclusion analysis (obtaining stage characteristics of authigenic minerals), isotope analysis, X-ray diffraction analysis, and other methods, the reservoir pore types of Huagang Formation were clarified, authigenic minerals were quantitatively analyzed to inverse porosity evolution process, and sandstone–tectonic interactions were examined. Consequently, geological development models for reservoirs of different origins in different layers of the Huagang Formation in the West Lake Sag have been established, which provide strong geological theoretical support for predicting high-quality reservoirs in the middle and deep layers of West Lake Sag.

2. Geological Setting

The West Lake Sag is a sub-depression of the Eastern Depression, located in the northeast of the East China Sea Shelf Basin, which orients north-east, is bordered on the east of the Marginal Uplift Fold Belt, on the west of the Yangtze River Depression and the Cape Uplift, and the southwest of the Yushan Uplift and Diaobei Depression, and approximates 5.9×10^4 km² [18,19]. West Lake Sag is a typical post-arc rift valley depression that has gone through three stages of tectonic evolution: fault subsidence, argument subsidence, and general subsidence, which can be separated into three regions based on its tectonic pattern and geological structure, such as western slope zone, center inversion tectonic zone, and eastern fault zone [20]. The Yuquan tectonics, the subject of this study, is a faulted anticline in the center of the central inversion tectonic belt. The Huagang Formation has experienced three significant tectonic movements (Figure 1b): during the deposition of Yuquan [21], Huagang [22], and Longjing formations [23]. The Eocene Series was uplifted and eroded exhibiting unconformity with substrata because the West Lake Sag was compressed by the Yuquan Movement dominated by shearing force, which was influenced by the Pacific Plate subduction direction alteration in the late Eocene [24]. The strong tectonic reversal occurred in the West Lake Sag as a result of fast subduction of the Philippine Plate to the northwest of the Asian Plate, which led to extensive stratigraphic folding, uplift, and denudation as well as retrograde reactivation of lower faults [25] and created the current tectonic configuration of the West Lake Sag.

During the rift stage, the depositional system of the West Lake Sag was dominated by bay-lake deposition. The depositional system of the Huagang, Longjing, Yuquan, and Liulang Formations was dominated by fluvial-lacustrine sedimentation. During the depositional period of the SanTan Formation and the Quaternary System, the West Lake Sag was in a state of general sedimentation, with lakes and shallow seas dominating [26]. The Huagang Formation of the research region is dominated by a braided river deltaic sedimentary structure [27]. In the shelf basin of the East China Sea, the stratigraphy of the West Lake Sag is comparatively complete. The following sedimentary periods were drilled from bottom to top: Yuquan Formation (N12y), Liulang Formation (N13l), Upper Eocene Santan Formation (N2s), lower Eocene (E2l), Upper-Middle Eocene Pinghu Formation (E2p), Oligocene Huagang Formation (E2h), Middle Eocene Longjing Formation (N11l), and Quaternary Pleistocene East China Sea Group (Qd). Approximately 15,000 m is the greatest thickness of the sedimentation [28]. This study focuses primarily on the Paleocene Oligocene Huagang Formation (E2h) stratigraphy. The stratigraphic age spans from 23.3 Ma to 32 Ma, and the seismic reflection layer is T30–T20. The Huagang Formation is separated into two parts: the lower Huagang Formation (H6–H12) and the Upper Huagang Formation (H1–H5). In the research area, every well that was drilled only reached the H7 horizon [4]. The Huagang Formation's sedimentary thickness varies from 1000 to 1800 m. Mudstone, muddy siltstone, siltstone, and fine sandstone make up the majority of its lithology, while coal seams visible in certain places. Positive grain sequence can be seen throughout the stratigraphic sequence. Mud is added in increasing amounts from the bottom up [29].

Currently, the A well area (Figure 1a) contains more than 100 billion cubic meters of identified tertiary reserves, of which more than 80 percent is tight sandstone gas. Furthermore, the Huagang Formation is the primary producing stratum, suggesting that this study area's rich sandstone reservoir presents significant opportunities for exploration and development [6].

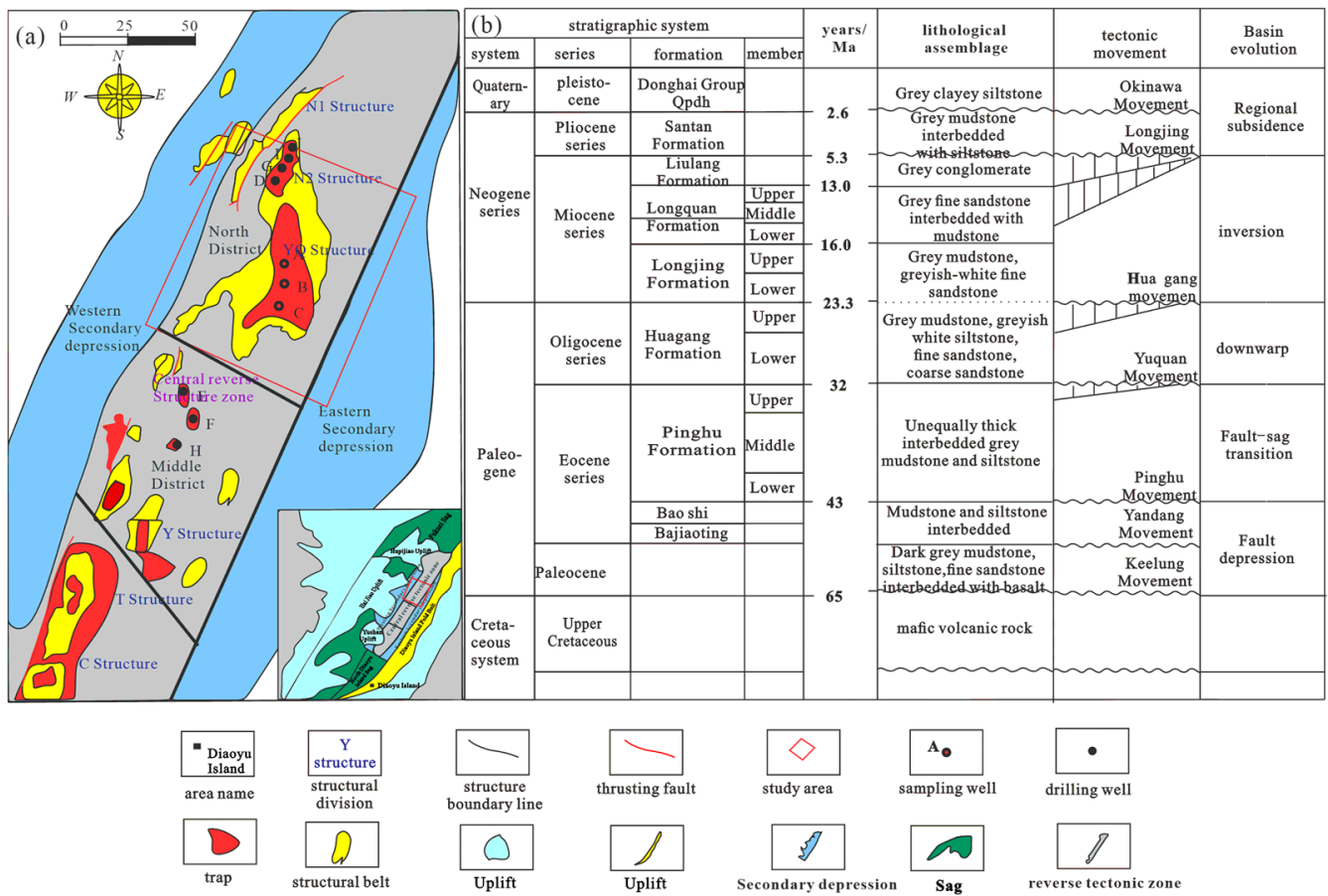


Figure 1. Location and stratigraphic table of the West Lake Sag tectonic belt in the East China Sea Basin. (a) Location map of the study area. (b) Stratigraphic composite histogram [28].

3. Samples and Methods

Seven wells in the Huagang Formation of the YQ Structure were chosen for sampling according to oil and gas display. Of these, 53 core samples were obtained and used to create 44 multifunctional sections and 29 plain thin sections (the sections were triple polished, blue-injected, and one-third dyed with alizarin red). Following that, a Leica DM2500 optical microscope fitted with a fluorescence emission unit was used for mineral identification, diagenesis analysis, and hydrocarbon injection characterization. The aforementioned experimental measures have been utilized to achieve the following specific tasks: 106 core porosity and permeabilities, 73 quantifications of rock minerals, and 73 quantifications of pore types.

One hundred core plugs 2.5 cm in diameter were washed with chloroform to clean up the pore fluids before physical property (porosity and permeability) analysis, and other physical property data were collected from CNOOC (China) Limited Shanghai Branch. In accordance with the national standard [30], porosity was tested through the alcohol saturation method and permeability was measured using a flowmeter by flowing air through the core.

Forty-two samples were selected for scanning electron microscopy (SEM) analysis to analyze the samples' rock mineralogy, diagenesis, and reservoir characteristics, to provide reliable experimental data and relevant experimental results to support the analysis of the formation and storage model. Minerals that could not be recognized by optical microscopy were subjected to electron microprobe examination and energy spectrum analysis (EDS).

The following are the names and models of the experimental tools used in the above mentioned experiments: model EPMA-1720 (JEOL Ltd., Tokyo, Japan.) for the electron

probe instrument, model TEAMTM XLT EDS electrocooled energy spectrometer, and model CARL ZEISS EVO MA15/LS 15 (Carl Zeiss AG, Oberkochen, Germany) for the scanning electron microscope. Aiming at the characteristics of the study area, such as multiple modes of mineral accumulation, multiple formation periods, small size of autochthonous minerals, and difficulty in identifying them, 27 thin sections were also selected for cathodoluminescence (CL) analyses to observe their luminescence characteristics.

Due to the fine particle size and difficulty in quantification of authigenic minerals, 49 representative samples were selected for mineral composition analysis (XRD) [31] based on microscopic identification results. The analysis instrument was a D/max-2500pc X-ray diffraction analyzer (Rigaku Corporation, Tokyo, Japan). On this basis, 40 samples were selected from 3 wells including A well, B well, and C well for constant and trace element detection [32,33]. The instruments are NexION 350X (PerkinElmer, Waltham, MA, USA) inductively coupled plasma mass spectrometer and PW2404 X-ray (PANalytical, Almelo, The Netherlands) fluorescence spectrometer (XRF).

To conduct timed and quantitative research on authigenic minerals in the study area, 10 typical fluid inclusions and micro-zone carbon and oxygen isotope multi-purpose slices were selected based on microscopic identification. Firstly, the uniform temperature and freezing point temperature were measured using a Linkam THMS-600 cold and hot stage (Linkam Scientific Instruments, Tadworth, UK) [34], and then the same sample was analyzed by mass spectrometry using an excitation light sampler [35]. At the same time, 17 samples were selected for in-situ and whole rock carbon and oxygen isotope analysis to obtain more information on the formation temperature and fluid characteristics of more authigenic minerals.

Constant and trace elements, in-situ micro region carbon and oxygen isotope composition, fluid inclusion temperature measurement, and scanning electron microscopy (energy spectrum) experimental analysis were completed at the CNOOC Experimental Center. The carbon and oxygen isotope composition testing of the entire rock was completed by the Key Laboratory of Natural Gas Accumulation and Development of PetroChina. The State Key Laboratory of Oil and Gas Reservoir Geology and Development Engineering of Chengdu University of Technology has completed thin section preparation and observation, porosity and permeability, whole rock mineral X-ray diffraction, cathodoluminescence and electron probe analysis.

4. Results

4.1. Rock Mineralogical Characteristics

According to the industry standard for rock slice identification (SY/T 5368-2000), the rock type of the Huagang Formation sandstone reservoir in the Yuquan structure is mainly feldspar lithic sandstone, (Figure 2). Based on the whole rock mineralogy, the quartz content of the Huagang Formation sandstone reservoir is between 46.1% and 86.8%, with an average of 71.9%, the feldspar content is between 5.6% and 29.8%, with an average of 16.58%, and rock fragments content ranges from 10% to 55%, with an average of 19.9% (Table 1). The Upper Huagang Formation mainly comprises potassium feldspar, while the lower Huagang Formation mainly comprises plagioclase. The particle size is mainly medium, followed by fine, with the Upper Huagang Formation slightly coarse than the lower one. There are three main types of cementation in the Huagang Formation: kaolinite, quartz, and carbonate. The cements in the Upper Huagang Formation are mainly kaolinite, followed by quartz and carbonate minerals, with a quartz content of 3.2% and a carbonate content of 4.3%. The Lower Huagang Formation is mainly composed of carbonate and quartz, with contents of 6.5% and 5.7%, respectively.

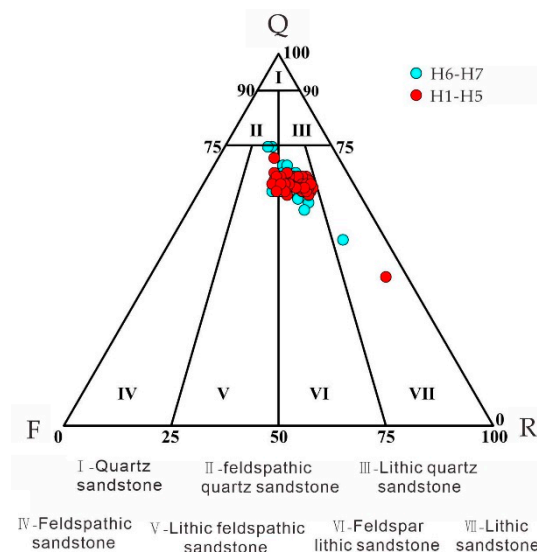


Figure 2. Rock-type triangle of the Huangang Formation of Yuquan Structure in the West Lake Sag.

Table 1. Whole rock X-ray diffraction analysis of sandstones in the Huangang Formation.

Well	Depth (m)	Content (wt%)					
		Quartz	Potassium Feldspar	Plagioclase	Calcite	Dolomite	Clay
A	2774	78.2	5.4	10.6	0.2	0.4	5.2
A	2804	83.0	5.7	6.9	0.5	0.6	3.3
A	3090	86.8	6.9	0	0.5	0.7	5.1
A	3122	85.7	7.1	0	0.7	0.6	5.9
A	3126	84.6	8.8	0	0.4	1.1	5.1
A	3126.5	85.4	6.6	0.3	0.5	0.9	6.3
A	3127.7	86.5	5.6	0	0.8	0.9	6.2
A	3128.9	84.8	7.3	0.3	0.6	1.0	6.0
A	3129.7	77.4	10.4	0.4	0.7	1.0	10.1
A	3130.9	75.5	11.1	0.3	1.3	1.5	10.3
A	3131.7	75.0	11.0	0.3	0.8	1.5	11.1
B	3720	71.9	6.0	16.4	1.0	0.5	4.2
B	3721.3	66.3	7.9	18.4	1.2	0.6	5.6
B	3722.3	72.7	6.7	14.4	1.0	0.6	4.6
B	3723.2	70.8	7.2	15.1	1.4	0.8	4.7
B	3724.3	74.4	5.0	13.9	0.3	0.6	5.8
B	3725.3	59.0	7.1	22.7	1.1	0.4	9.0
B	3726.3	42.8	7.1	14.5	31.5	1.0	3.1
B	3726.6	50.9	3.7	15.7	1.1	3.3	25.3
B	3730.8	54.8	2.3	17.0	2.6	4.1	19.2
B	3734.8	46.1	1.1	10.8	6.8	4.8	30.4
B	4418.4	72.1	2.7	18.9	0.2	0.7	5.4
B	4419.4	67.4	3.7	20.7	1.0	0.3	6.9
B	4420.4	72.8	3.4	18.4	0.7	0	4.7
B	4421.4	74.0	2.3	18.5	0.2	0.3	4.7
B	4422.4	75.0	2.8	17.6	0.3	0.7	3.6
B	4423.4	68.0	5.6	15.1	0.2	0	11.1

4.2. Pore Characteristics

4.2.1. Pore Type

The Huangang Formation sandstone in the Yuquan structure has developed cemented and metasomatic carbonate dissolution pores, particle dissolution pores such as feldspar and igneous rock debris pores, intercrystalline pores, and residual primary intergranular pores. The Upper Huangang Formation is mainly composed of cemented and metasomatic

carbonate dissolution pores, followed by particle dissolution pores, and the Lower Huagang Formation is mainly composed of particle dissolution pores.

Cementitious and metasomatic carbonate dissolution pores, some of which are super large pores, have irregular pore edges and a few filling minerals with pervasive carbonate residuals (Figure 3a,b). Particle dissolution pores are often filled with dissolution products such as kaolinite and illite (Figure 3a–c,e,f), which are easy to distinguish from carbonate dissolution pores.

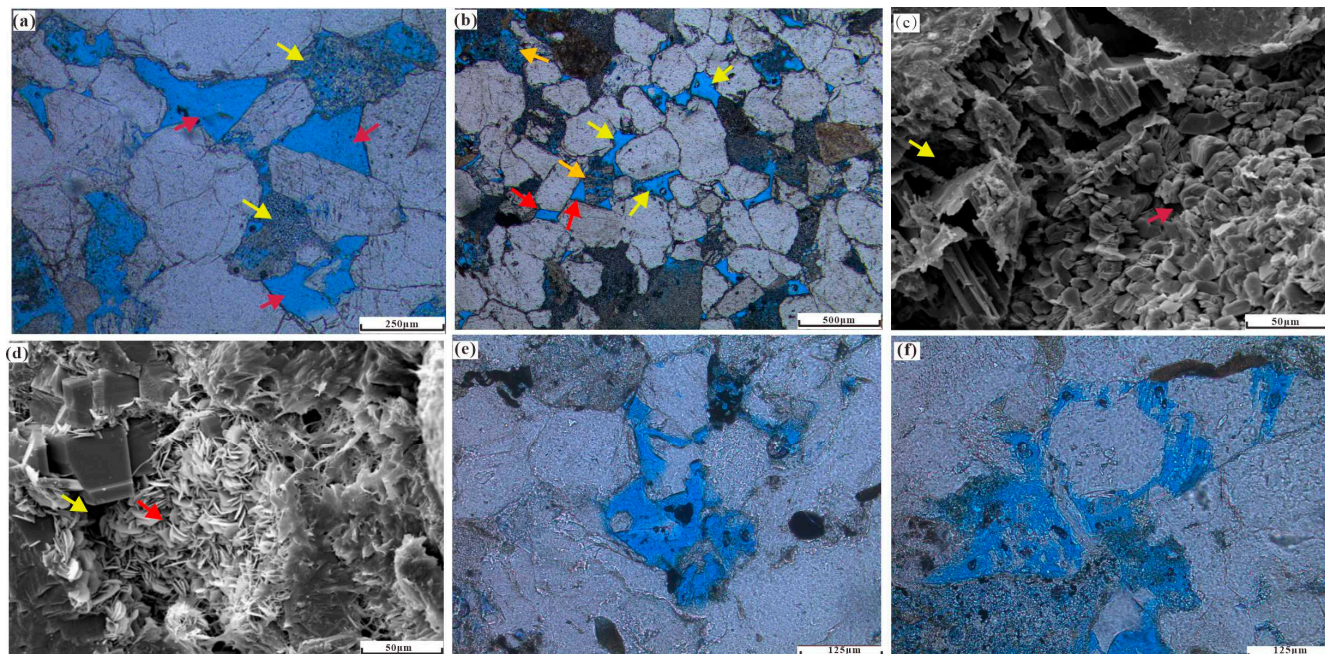


Figure 3. Pore types of the Huagang Formation of the Yuquan Structure in the West Lake Sag. (a) Carbonate dissolution pores (red arrow) and feldspar dissolution pores (yellow arrow), A well, Upper Huagang Formation, 3135.9 m, PPL. (b) Intergranular carbonate dissolution pores (yellow arrow), feldspar dissolution pores (orange arrow), and a small amount of residual primary pores (red arrow), A well, 3125.9 m, Upper Huagang Formation, PPL. (c) Feldspar dissolution pores (yellow arrow) and kaolinite intergranular pores (red arrow), A well, Upper Huagang Formation, 3134.9 m, SEM. (d) Chlorite intergranular pores (red arrow) and residual throats (yellow arrow), A well, Lower Huagang Formation, 4143 m, SEM. (e) Particle dissolution pore, C well, Lower Huagang Formation, 3989.8 m, PPL. (f) Particle dissolution pore, C well, Lower Huagang Formation, 3989.8 m, single polarized light (PPL).

The residual primary intergranular pore belongs to a type of intergranular pore, characterized by flat pore edges, commonly known as angular pore (Figure 3b). It needs noticing that dissolved pores of intergranular cement often appear among particles which are always considered as intergranular pores by some geology researchers. However, the genesis of dissolved pores of intergranular cement is significantly different from residual primary intergranular pores, so it is necessary to accurately distinguish these two different pore types. Unlike straight edges of residual primary intergranular pores, cement dissolution pores exhibit irregular edges (Figure 3a,b) and obvious cement residuals.

Although intercrystalline pores are one of the most common pore types in the study area, their contribution to porosity is not significant. The main intergranular pores are kaolinite and illite intercrystalline pores, followed by chlorite and quartz intercrystalline pores. Intercrystalline pores of the Upper Huagang Formation are mainly composed of kaolinite intercrystalline pores, while those of the Lower Huagang Formation mainly consist of illite and chlorite intercrystalline pores (Figure 3c,d).

4.2.2. Pore Combination Characteristics

According to the main pore development characteristics of Upper Huagang Formation reservoirs in the Yuquan structure, the following types of pore combination types can be divided: (1) Carbonate dissolution pore + particle dissolution pore type is dominated by carbonate cement dissolution pores mainly developed in the Upper Huagang Formation, followed by feldspars, which is the main pore combination type in the best reservoirs. (2) Carbonate dissolution pore types are mainly formed by carbonate cement dissolution which is mainly developed in sandstone with high quartz content and low feldspar content in the Huagang Formation. (3) Particle dissolution pore + intercrystalline pore type is dominated by feldspar particle dissolution, followed by intercrystalline pores, which can be divided into three sub-types according to crystal types: particle dissolution pore + kaolin intercrystalline pore, particle dissolution pore + illite intercrystalline pore, and particle dissolution pore + chlorite intercrystalline pore, and the first sub-type is mainly distributed in the Upper Huagang Formation, while the latter two mainly developed in the Lower Huagang Formation.

4.3. Physical Characteristics

There are significant differences in physical properties between different layers of the Huagang Formation. The peak porosity of the Upper Huagang Formation is 15%–20%, with an average of 16.7%, while the peak porosity of the Lower Huagang Formation is only 5%–10%, with an average of 7.5%. The permeability of the Upper Huagang Formation is mainly in the range of $1\text{--}10 \times 10^{-3} \mu\text{m}^2$, while the permeability of the sandstone reservoir in the Lower Huagang Formation is less than $1 \times 10^{-3} \mu\text{m}^2$. The correlation between porosity and permeability in the Upper Huagang Formation is significantly better than that in the Lower Huagang Formation, reflecting the difference in pore composition between the two. In summary, the Huagang Formation reservoir is mainly composed of low-permeability and tight sandstone reservoirs [36], and the physical properties of the Upper Huagang Formation are better than those of the Lower Huagang Formation (Figure 4).

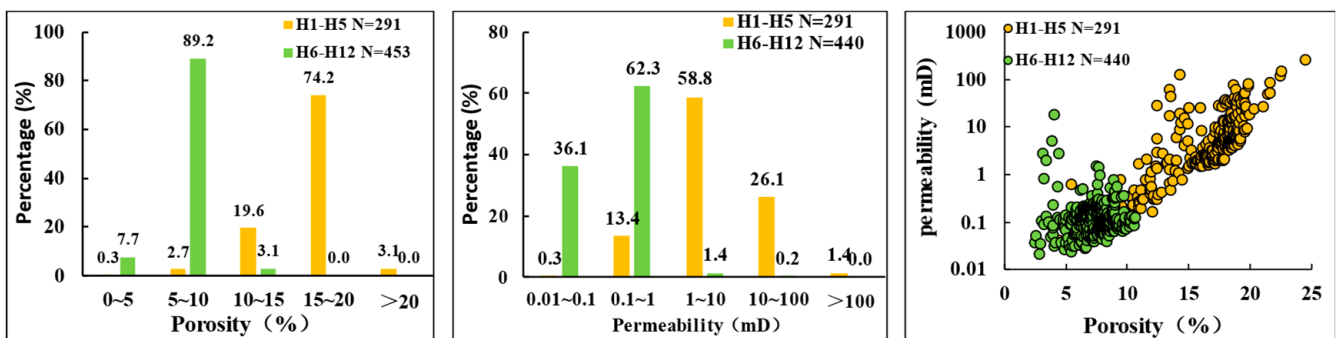


Figure 4. Physical Characteristics of the Huagang Formation of Yuquan Structure in the West Lake Sag.

4.4. Type of Diagenesis

4.4.1. Compaction Effect

The mechanical compaction of the overlying strata combined with the tectonic compression, especially the strong compression during the inversion period, is the main factor leading to porosity loss in the Huagang Formation [21]. At present, low porosity sandstones generally show characteristics such as linear contact of detrital particles, locally partial concave-convex contact (Figure 5a), bending deformation of sheet-like minerals, particle directional arrangement, wavy extinction of detrital quartz, and some particle cracks caused by mechanical compaction, reflecting strong mechanical compaction. Some sandstones have undergone pressure dissolution, showing concavo-convex contact and stylolites in quartz particles (Figure 5b).

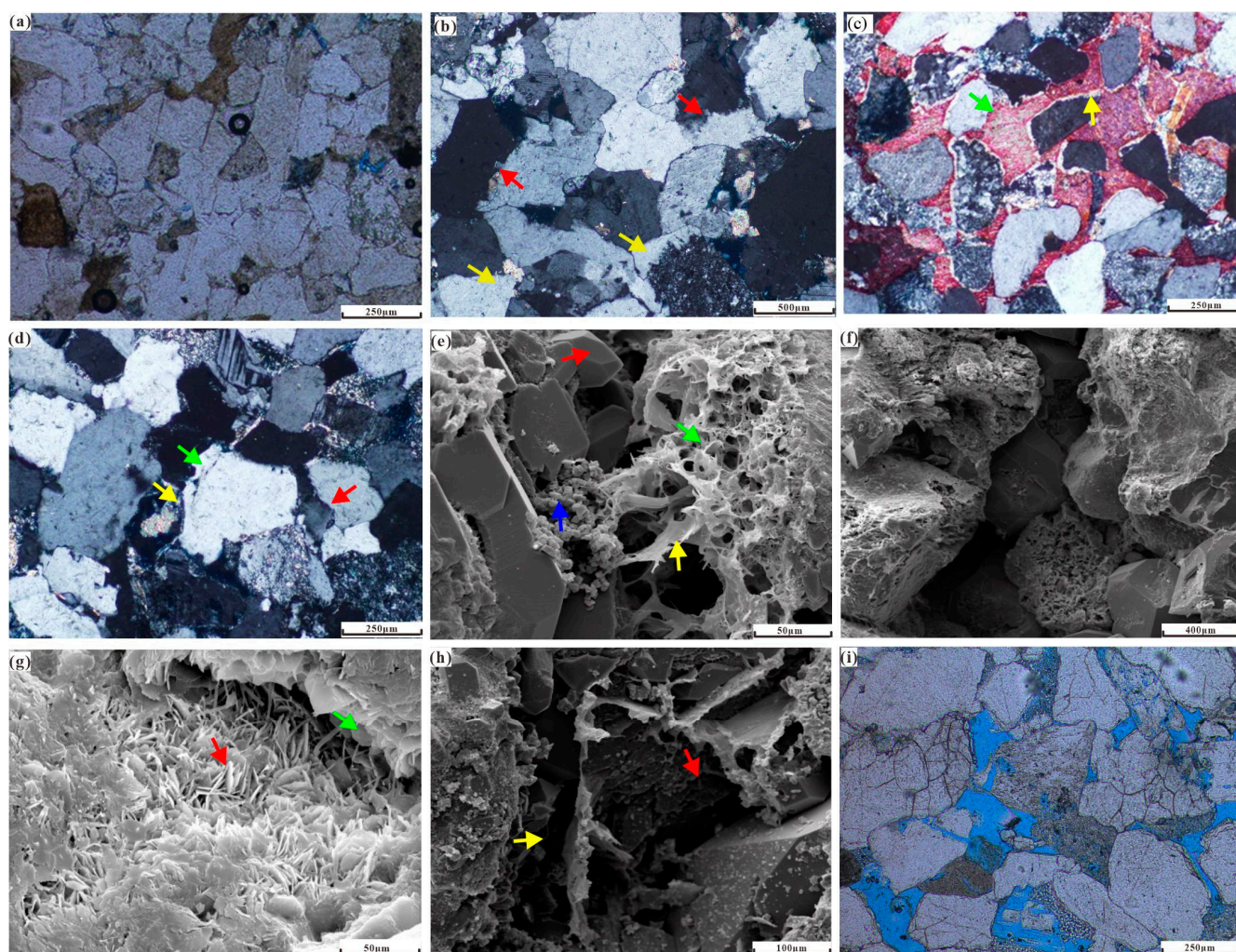


Figure 5. Microscopic characteristics of diagenetic in the Huagang Formation sandstone of the Yuquan Structure. (a) Particle line, concavo-convex contact, A well, Lower Huagang Formation, 3973.4 m, PPL. (b) Particle concavo-convex contact, suture contact (red arrow), and authigenic quartz (yellow arrow), A well, Lower Huagang Formation, 4424.4 m, XPL. (c) Illite (yellow arrow) and calcite cement (green arrow) in sandstone, stained with Alizarin Red, A well, Upper Huagang Formation, 3570 m, XPL. (d) Multiphase authigenic quartz from early (red arrow), middle (green arrow) to late (yellow arrow), A well, Lower Huagang Formation, 3961 m, XPL. (e) Honeycomb-like illite mixed layer (green arrow), filamentous illite (yellow arrow), authigenic quartz (red arrow), and kaolinite (blue arrow), A well, Upper Huagang Formation, 3126.9, SEM. (f) Formation of honeycomb-shaped dissolution pores by dissolution of feldspar particles, A well, Upper Huagang Formation, 2911 m, SEM. (g) Chlorite filling the pores (red arrows) and the chlorite at the particle edges (green arrows), A well, Lower Huagang Formation, 4143 m, SEM. (h) Intergranular carbonate dissolution residue (red arrow) and feldspar dissolution (yellow arrow), A well, Upper Huagang Formation, 3136.4 m, SEM. (i) Irregular crack development on particles, A well, Lower Huagang Formation, 3135.9 m, PPL.

4.4.2. Authigenic Minerals Precipitation

During the burial process of the Huagang Formation sandstone of the Yuquan Structure, various minerals were precipitated along with changes in the diagenetic environment. Based on the microscopic occurrence characteristics, the sequence of mineral precipitation can be identified, and multiple precipitation periods of the same mineral can also be distinguished. The authigenic minerals during the diagenesis process of Huagang Formation sandstone include three phases of quartz, two phases of illite, two phases of calcite, two

phases of chlorite, one phase's kaolinite, and one phase's Imon mixed layer (Figure 5c–h), as well as a small amount of pyrite and limonite.

4.4.3. Dissolution

Dissolution in the Huagang Formation mainly occurs in carbonate cements and detrital feldspars rock fragments dissolution, and carbonate dissolution is the most important in the Upper Huagang Formation, while feldspar dissolution is the most important in the Lower Huagang Formation (Figures 3 and 5c–h).

4.4.4. Tectonic Rupture

The Huagang Formation underwent multiple stages of tectonic movement, such as the compression and depression stage from the late Eocene to the late Miocene [4], which resulted in lots of fractures forming (Figure 5i).

5. Discussion

5.1. Chronological and Quantitative Analysis of Pore Evolution

5.1.1. Porosity Evolution

Using thin-section microscopic observation and scanning electron microscopy analysis, the sequence of mineral precipitation during the diagenesis process was identified. The earliest diagenetic mineral was the first stage of quartz overgrowth, followed by leaf-shaped chlorite attached to the surface of particles (Figure 6a). Iron calcite always occurs in the zones of point-to-line contact and grows on the overgrowth quartz, indicating its formation as early but later than the first stage of overgrowth quartz (Figure 6b,g). There are two types of occurrence modes of illites: bridging illites grow in the pores and throats, which formed after carbonate dissolution (Figure 6c), and needle-like illites fill in the pores which often correlate with feldspar dissolution. Pore-filling cements like kaolinite, illite, and quartz can be seen in feldspar dissolution pores. Kaolinite is not developed in carbonate dissolution pores adjacent to feldspar dissolution pores, indicating that carbonate dissolution occurs later than feldspar dissolution (Figure 6d,h,i). In feldspar dissolution pores, kaolinite grows on pore-filling quartz, and illite adheres to kaolinite, which shows the precipitation order of feldspar dissolution–quartz–kaolinite–illite–carbonate dissolution (Figure 6e). The earliest dissolution occurred in the Lower Huagang Formation at the end of the sedimentation of the Huagang Formation. The second stage of dissolution mainly relates to the atmospheric water caused by the reversal tectonic movement, mainly developed in the Upper Huagang Formation, especially in the areas with developed faults and highlands, which is characterized by carbonate dissolution and followed by feldspar dissolution. The third stage of dissolution is related to the further burial of the Huagang Formation and the release of acidic fluids from the underlying source rocks after the tectonic reversal movement, which mainly occurred in the Lower Huagang Formation (Figure 6e,f).

The temperature distribution of the inclusions in the last three stages of authigenic quartz is in three temperature ranges: 80–120 °C, 120–160 °C, and above 160 °C. The four stages of authigenic quartz identified by microscopic microscopy were matched. Based on the paleo geothermal gradient of 3.7 °C/100 m and burial history characteristics of the Huagang Formation in the research area [37], authigenic quartz in the sandstone of Huagang Formation of the Yuquan structure mainly formed in the late sedimentation of the Huagang Formation, the late sedimentation of the Longjing Formation, the early sedimentation of the Yuquan Formation, and the late sedimentation of the Yuquan Formation. Some authigenic quartz inclusions had higher temperatures, which may be related to the abnormally high temperature caused by strong tectonic compression during the inversion period. The diagenesis sequence indicates that the most widely distributed poikilitic calcites in the study area formed after the first quartz overgrowth, before the detrital particles became point-to-line contact.

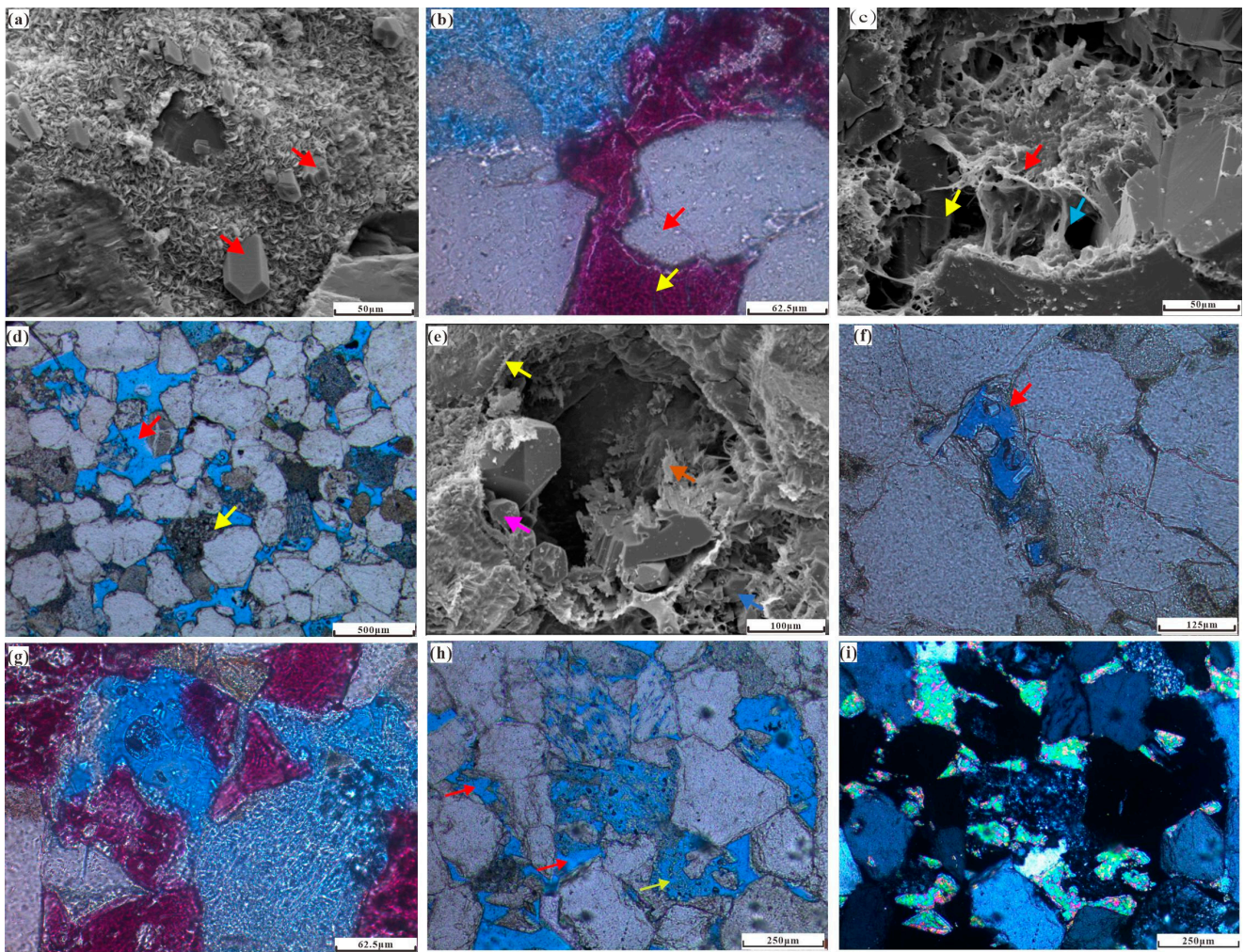


Figure 6. Microsympiosis of diagenetic minerals and dissolution characteristics in the Huagang Formation sandstone of the Yuquan Structure. (a) The authigenic chlorite on the surface of particles occurs later than authigenic quartz (red arrow), A well, Upper Huagang Formation, 3141 m, SEM. (b) Enlarged quartz (red arrow) earlier than cemented iron calcite (yellow arrow), Upper Huagang Formation, A well, 3130.4, PPL. (c) Early envelope illite (red arrow); carbonate dissolution of cementation later than illite (yellow arrow); bridged illite dissolved later than carbonate (blue arrow), A well, Upper Huagang Formation, 3947.3 m, SEM. (d) Feldspar dissolution pores and kaolinite in their pores (yellow arrow); No kaolinite in carbonate dissolution pores (red arrow), A well, 3125.9 m, Upper Huagang Formation, PPL. (e) Residual envelope illite at the edge of feldspar dissolution pores (yellow arrow); fill the solution with authigenic quartz (rose red arrow); Illite (orange-yellow arrow); residual carbonate from intergranular dissolution (blue arrow), A well, Lower Huagang Formation, SEM. (f) Authigenic quartz in feldspar dissolution pores, A well, Lower Huagang Formation, 3978.9 m, PPL. (g) Quartz enlargement; cementation and replacement with iron calcite; dissolution; filling with illite and kaolin (from early to late), Upper Huagang Formation, A well, 3130.4, PPL. (h,i) Feldspar dissolution and carbonate dissolution later than Feldspar dissolution (red arrow); Kaolin, a product of feldspar dissolution, is only distributed in feldspar dissolution pores (yellow arrow), A well, Upper Huagang Formation, 3127 m, (h: PPL, i: XPL).

Based on the carbon and oxygen isotope values of poikilitic calcites, representing penecontemporaneous diagenetic fluid, Z-values were calculated based on Keith and Weber's (1964) salinity index calculation formula [38] and salinity (S), according to the Pacific seawater's fitting equation between $\delta^{18}\text{O}$ value and salinity. About 88.2% of the samples have a Z-value less than 120 and salinity S ranges from 1.02% to 2.52%, indicating

that the early diagenetic (or sedimentary) fluids were mainly saline freshwater. Therefore, taking fresh atmospheric water from coastal areas $\delta^{18}\text{O}_{\text{SMOW}} = -5\text{‰}$ as precipitation fluid for calcite $\delta^{18}\text{O}_{\text{SMOW}}$ value [39] and using the calcite water fractionation equation [40], the precipitation temperature range of 19–105 °C of crystalline calcites was calculated. Based on the classification criteria for the diagenetic stages of clastic rocks [41], they can be divided into four phases from early to late including <40 °C, 40–60 °C, 60–80 °C, and 80–104 °C, corresponding to syngenes, phase A of early diagenesis, phase B of early diagenesis and phase A of meso diagenesis. The development stages of crystalline calcite are mainly syngenes and phase A of early diagenesis. The metasomatic calcites are divided into three stages including 40–60 °C, 60–80 °C, and 80–105 °C, corresponding to phase A of early diagenesis, phase B of early diagenesis, and phase A of meso diagenesis (Figure 7).

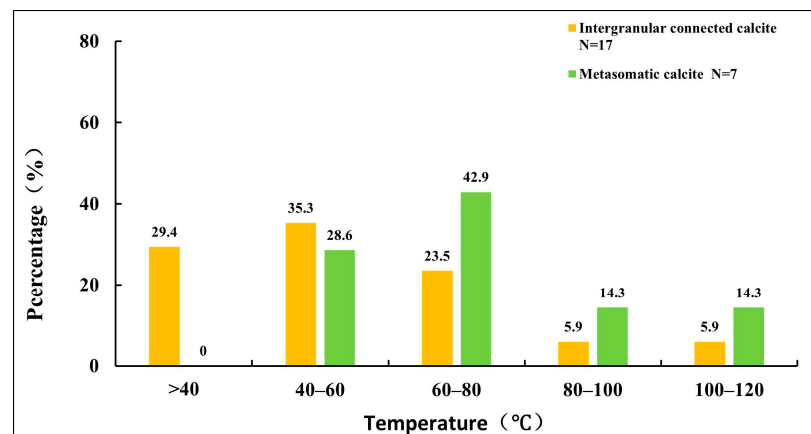


Figure 7. Calculation of temperature distribution histogram for oxygen isotopes of calcite with different occurrences in the sandstone of the Huagang Formation of the Yuquan structure.

According to the maximum temperature of fluid inclusions in the study area of less than 170 °C (Figure 8) and quantitative analysis of X-ray diffraction of clay minerals of mudstone at a burial depth of 3750–4200 m in Well A and B, the S% in the I/S mixed layer is less than 20%. The S% of 4400 m in Well B is about 10%, and the corresponding rock-eval temperature (T_{max}) is only 415 °C. Consequently, it can be seen that the latest diagenetic stage of the sandstone reservoir of the Huagang formation of the Yuquan Structure is phase B of mesodiagenesis, and most sandstone reservoirs experienced phase A of mesodiagenesis. Based on the above achievements, a diagenetic sequence was established for the sandstone reservoir of the Huagang formation of the Yuquan Structure (Figure 9).

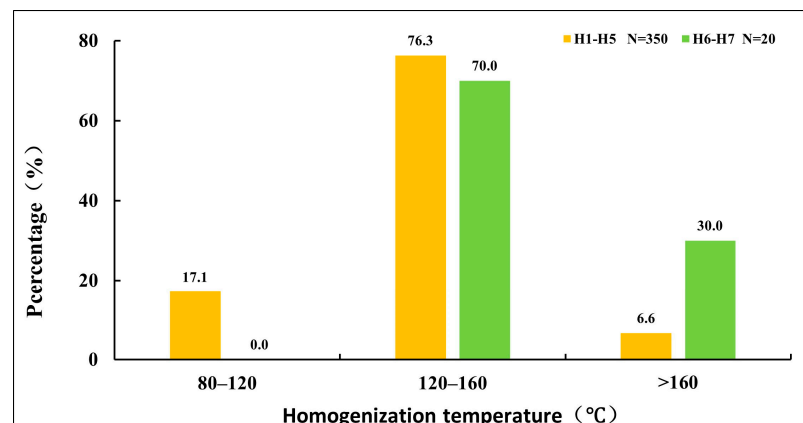


Figure 8. Temperature distribution of inclusions in authigenic quartz of the Huagang Formation sandstone in the Yuquan Structure.

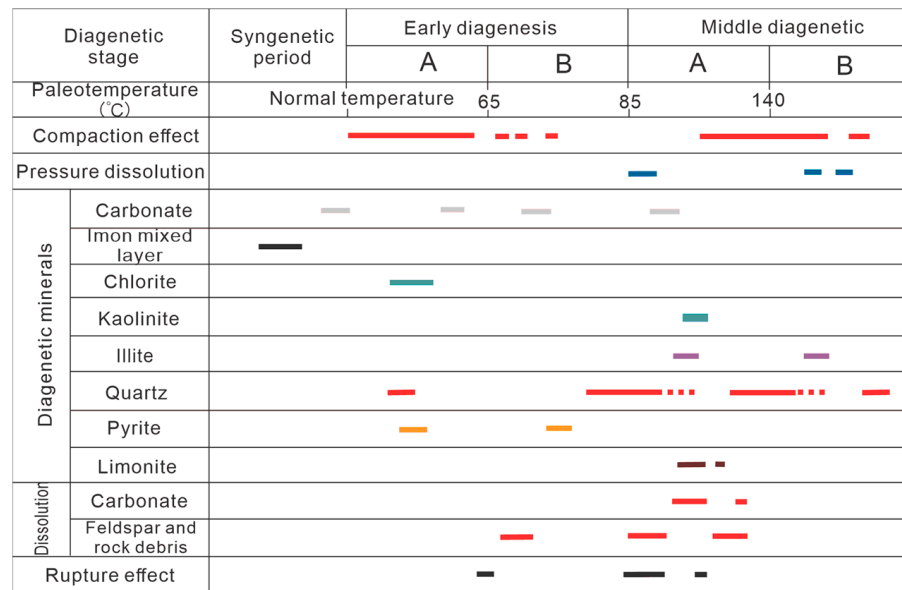


Figure 9. Diagenetic symbiosis of the Huagang Formation sandstone reservoir in the Yuquan Structure.

5.1.2. Quantitative Inversion of Porosity

The quantitative evolution of porosity includes initial porosity evolution in the sedimentation stage, evolution of pores formed during burial, amount of mineral precipitation that damages pores, and porosity formed by burial dissolution. The quantitative evolution of initial porosity and newly formed pores during diagenesis during burial is mainly based on mechanical compaction law and typical development characteristics of porosity in critical diagenesis, and an initial porosity-depth inversion model is established to determine the porosity reduced by mechanical compaction in each stage. The amount of porosity damage caused by precipitated minerals during the burial process is calculated by the number of authigenic minerals with different occurrences through the line counting method on 70% to 80% of each thin section under the microscope. The dissolution porosity was quantitatively analyzed by the line counting method to obtain the proportion of particle dissolution pores, carbonate dissolution pores, etc. (Tables 2 and 3).

Table 2. Pore and diagenetic mineral composition of sandstone reservoir in the Huagang Formation of the Yuquan Structure.

Pore	Pore Type	Reservoir Type		
		Carbonate Dissolution Pore + Particle Dissolution Pore Type	Carbonate Dissolution Pore Type	Particle Dissolution Pore Type
Pore(%)	Carbonate dissolution pore type	10.0	10.0	2.0
	Particle dissolution pore type	6.2	2.4	5.5
	Residual intergranular pore	1.8	0.6	1.0

Table 3. Diagenetic mineral composition of sandstone reservoir in the Huagang Formation of the Yuquan Structure.

Authigenic Mineral	Mineral Period	Reservoir Type		
		Carbonate Dissolution Pore + Particle Dissolution Pore Type	Carbonate Dissolution Pore Type	Particle Dissolution Pore Type
Quartz	Phase 1	1.0	1.0	0.5
	Phase 2	2.0	1.0	0.7
	Phase 3	0.0	0.0	3.9
Illite/smectite mixed layer (%)		1.8	1.4	1.5
Chlorite (%)	Phase 1	0.0	0.0	1.4
	Phase 2	0.0	0.0	0.4
Kaolinite (%)		6.3	1.9	0
Illite(%)	Phase 1	0.0	0.0	0.7
	Phase 2	0.5	0.5	1.0
Carbonate (%)	Cementation	10.0	11.0	4.0
	Metasomatism	3.5	2.0	1.0

5.1.3. Evolution Characteristics of Reservoir Pores

Based on the paragenetic relationship of the main diagenetic processes in porosity evolution the key diagenetic periods, and quantitative characteristics of various diagenetic processes on the reservoir, combined with ancient geothermal gradients in the study area, the chronological and quantitative evolution characteristics of porosities in the above three types of reservoirs of the Huagang Formation in the Yuquan structure, as well as their relationship with structural evolution were obtained (Figure 10).

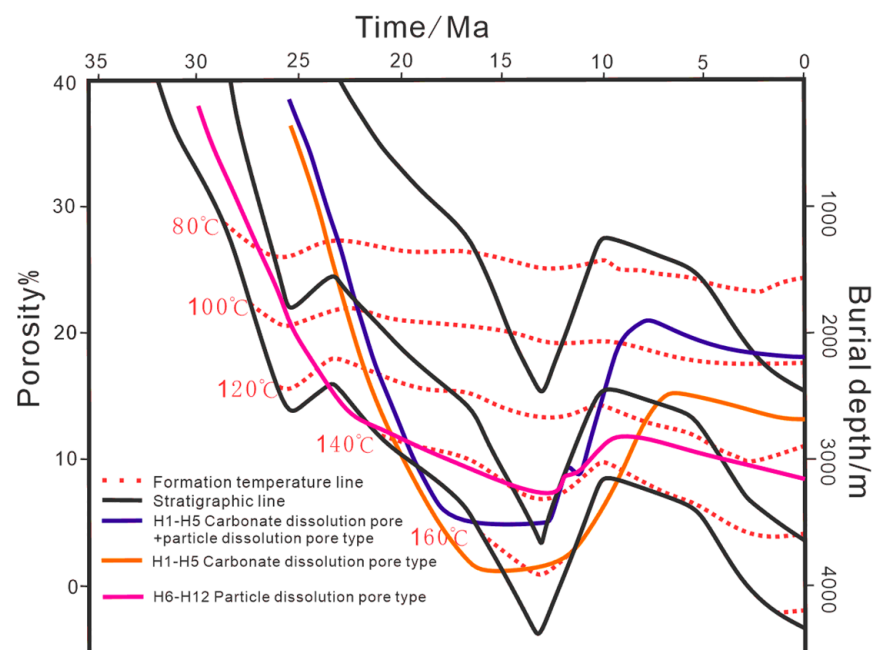


Figure 10. Coupling relationship between pore evolution and structural evolution of sandstone reservoir in the Huagang Formation of the Yuquan Structure.

It can be seen that the carbonate dissolution pore + particle dissolution pore type reservoir in the Upper Huagang Formation lost porosity due to mechanical compaction and carbonate cementation at the end of sedimentation of the Longjing Formation, and the porosity decreased to 5.8%. At the early stage of the Longjing Movement, the fault transported acidic fluids discharged from the evolution of the underlying source rock into the reservoir rock, resulting in intense dissolution of feldspar, and the porosity improved to 9%. In the middle stage of the Longjing Movement, a strong reverse tectonic movement formed a large number of fault fractures, uplifted the Upper Huagang Formation, and formed good connectivity between atmospheric water and sandstone, resulting in strong dissolution of early precipitated carbonates and the formation of good reservoirs with porosity close to 20%. The main difference in porosity evolution between the carbonate dissolution pore type reservoir and the carbonate dissolution pore + particle dissolution pore type reservoir is that the carbonate cementation is slightly stronger in the late sedimentary period of the Longjing Formation, especially in the area of underdeveloped hydrocarbon source faults during the early stage of the Longjing Movement, where the degree of feldspar dissolution is significantly reduced. As a result, dissolution products like kaolinite are significantly lower than in the latter. Therefore, the porosity improvement of the early stage of the Longjing Movement is very small, which directly leads to the current porosity of the reservoir is only 13%, significantly lower than that of the carbonate dissolution pore + particle dissolution pore type reservoir. The particle-dissolution pore-type reservoir in the Lower Huagang Formation was developed under tension force in some areas during the late sedimentation period of the Huagang Formation, providing a pathway for acidic fluids to enter the reservoir. The porosity can reach about 15% due to feldspar dissolution. However, in the late sedimentation period of the Longjing Formation, due to the compaction of the overlying strata, the porosity decreased to 9.5%. In the early to middle stages of the Longjing Movement, the porosity decreased to less than 4% due to the influence of tectonic compression and the formation of more developed pressure-solution quartz. However, the strong reversal in the middle and late stages of the Longjing Movement resulted in the formation of well-developed faults and fractures, causing the dissolution of some feldspar and the porosity increased to 8.5%. If the sandstone of the Lower Huagang Formation has a large fault and good connectivity with the underlying source rock at the late sedimentation stage of the Huagang Formation, more acidic fluids will enter the reservoir, leading to stronger dissolution of feldspar at this stage, and further reducing the amount of pressure dissolved quartz. If there are more developed faults during the strong inversion period, then the feldspar dissolution pores in that period are also more developed, thus forming a good reservoir with a current porosity close to 15%.

5.2. Main Controlling Factors for Reservoir Development

5.2.1. Temporal and Spatial Configuration Relationship between Reservoir Rock and Tectonics Being the Most Crucial Factor

The Yuquan structure has roughly gone through three important stages of tectonic variations: extension and depression, strong compression, and compression adjustment (Figure 11). From the sedimentation period of the Pinghu Formation to the sedimentation period of the Huagang and Longjing Formations, the main transition period was from the early strong extensional background to the depression period of the Huagang Formation. After the sedimentation of the Upper Huagang Formation, the fault activity did not stop until the sedimentation period of the Longjing Formation. Faults of the period mainly developed in the Pinghu Formation and extended upwards to the Lower Huagang Formation, causing feldspar dissolution in the sandstone distributed in the fault development area of the Lower Huagang Formation and partial particle dissolution.

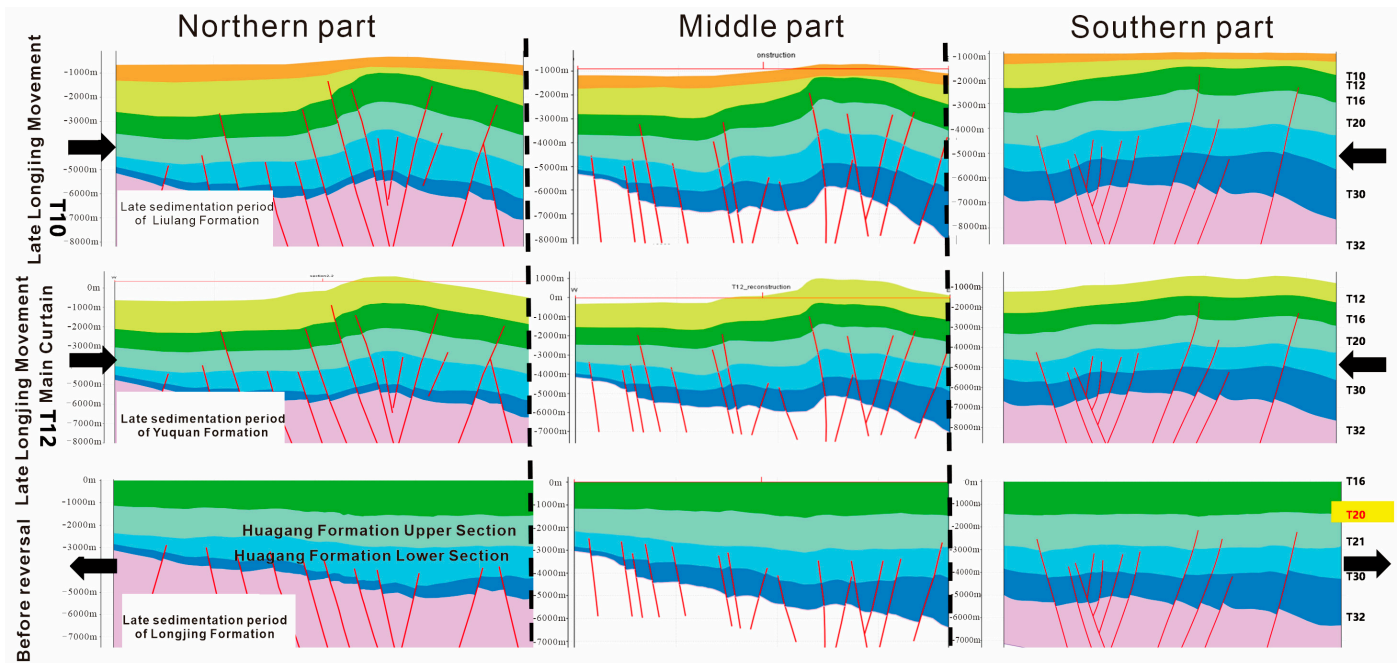


Figure 11. Tectonic evolution characteristics of the Huagang Formation of the Yuquan structure after sedimentation (revised after Wang [24]).

The Huagang Formation experienced the strongest compression in the early and middle stages of the Longjing Movement which occurred at the end of the sedimentation period of the Yuquan Formation. The precursor faults were generally activated and extended to the Yuquan Formation, accompanied by a series of regulating faults and a large reverse anticline. The core of the anticline suffered from large-scale erosion, resulting in good connectivity between the sandstone of the Upper Huagang Formation and atmospheric water, as well as underlying acidic fluids, through faults, unconformity surfaces, etc. This led to the strong dissolution of carbonate and feldspar in the Upper Huagang Formation and formed a good reservoir with a porosity of about 20%. However, the Lower Huagang Formation due to its deeper burial, had poor communication with atmospheric water, which also led to poor porosity. This is also the main reason for the lower porosity of the Lower Huagang Formation compared to the Upper Huagang Formation. Carbonate dissolution pores are particularly developed in the Upper Huagang Formation, while they are poorly developed in the Lower Huagang Formation. Authigenic kaolinite is mainly distributed in the Upper Huagang Formation, and there are few in the Lower Huagang Formation, all of which indicate that the porosity origin of the Upper Huagang Formation is mainly attributed to the reversal structure of this period. The late stage of the Longjing Movement that occurred in the sedimentation period of the Liulang Formation was a compression adjustment stage, during which the main controlling fault of the reverse anticline was still active. Therefore, in these fault development areas, the underlying acidic fluid entered the Lower Huagang Formation and dissolved feldspar, carbonate, etc. However, due to the dense nature of the Lower Huagang Formation before this dissolution period, the degree of dissolution was not strong, and the improvement of the sandstone's physical properties was limited. Only in the sandstone with early chlorite, due to the relatively good throat, provided a good channel for dissolution in this period, and a good reservoir formed.

5.2.2. Early Precipitation of Carbonates Laying the Material Foundation for Reservoir Formation in the Upper Huagang Formation

In the early burial stage of the Upper Huagang Formation, a large amount of carbonate minerals such as calcite and iron calcite were precipitated, mainly occurring as intergranular pore-filling, followed by metasomatic (Figure 6), resulting in severe porosity damage. The sandstone porosity is only about 5%, and in some strongly cemented areas,

the porosity of sandstone is 0%. However, the carbonate minerals indirectly preserve the volume between particles. The reverse of the Yuquan Structure made retrogressive dissolution of carbonates occupying intergranular space (Figures 3 and 6). Therefore, early carbonates in the Upper Huagang Formation of the Yuquan Structure can be regarded as preservation diagenesis [42], which occupied the intergranular space in the early stage and underwent dissolution in the later stage.

5.2.3. Early Weak Alkaline Environment and Abundant Detrital-Feldspar Being the Foundation for Reservoir Formation of the Lower Huagang Formation

Sandstones with relatively good physical properties in the Lower Huagang Formation of the Yuquan Structure generally have chlorite on the particle surface, and the content of chlorite is positively correlated with porosity. Microscopic characteristics show that the formation of chlorite in this period was early, mainly formed at the time of point-line contact. Energy spectrum analysis results show that chlorite in this period has high levels of Fe_2O_3 and MgO (Figure 12). The fine-grained sandstones in the Huagang Formation in the study area have well-developed mica and I/S mixed clay. These minerals are prone to hydration and release iron ions, magnesium ions, etc., in the contemporaneous period, and under the combined action of a weak alkaline sedimentary environment in the Lower Huagang Formation, they are prone to form chlorite. The chlorite on the surface of particles inhibits the formation of other diagenetic minerals during early burial periods, such as the early overgrowth quartz. The chlorite on the surface of particles makes sandstone have better permeability for a long burial time. It is beneficial for the dissolution of detrital feldspar in the fault development zone during early to middle burial periods and it also further weakens the strength of pressure dissolution of particles due to tectonic compression during the period of structural inversion, thus forming relatively good reservoirs. In both the Upper Huagang Formation and Lower Huagang Formations, particle dissolution pores are formed by the dissolution of feldspar and rock debris, especially in the sandstone of the Lower Huagang Formation. The particle dissolution pores in the Lower Huagang Formation account for 65% of the total pores. It can be seen that to form reservoirs of the Lower Huagang Formation, the source material needs to have a relatively rich content of feldspar. The relationship between feldspar and porosity (Figure 13) also indicates that one of the prerequisites for reservoir formation in the Lower Huagang Formation sandstone is a high-content feldspar source.

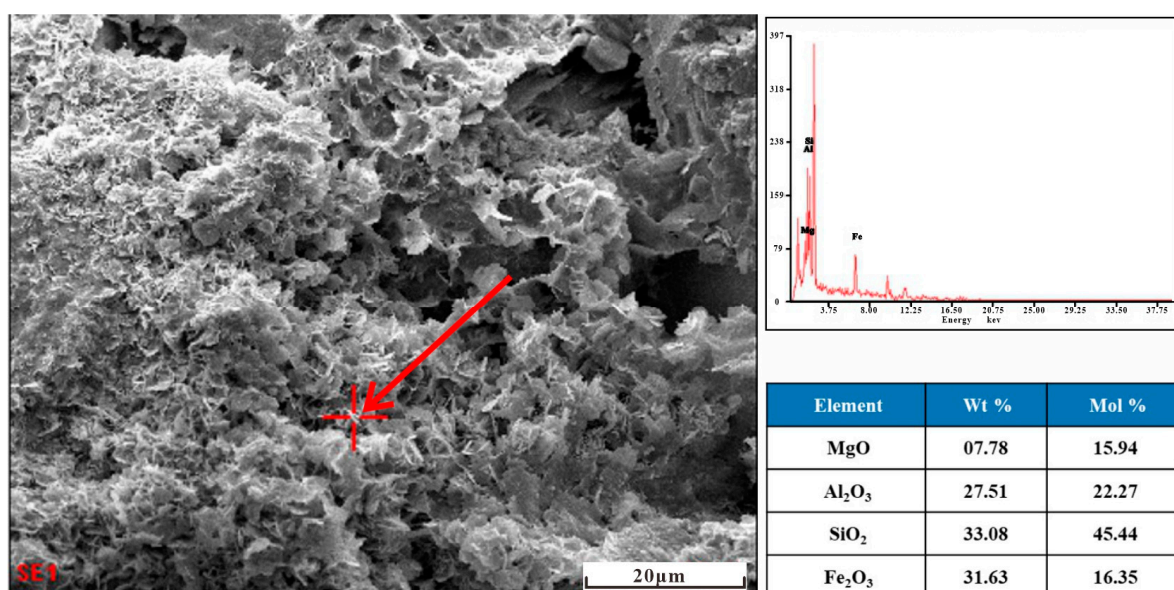


Figure 12. Characteristics of surface chlorite and its energy spectrum components in the Lower Huagang Formation of the Yuquan Structure.

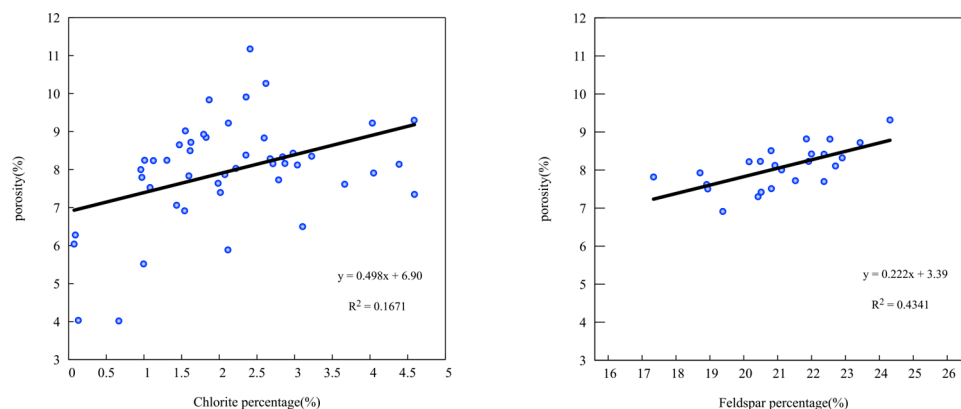


Figure 13. Relationship between content and porosity of authigenic chlorite and clastic feldspar in the Lower Huagang Formation of the Yuquan Structure.

5.3. Reservoir Formation Model

5.3.1. Carbonate Dissolution Pore + Grain Dissolution Pore Type

During the initial deposition of clastic particles, the original intergranular volume is large. In the early stages of sedimentation, a large amount of intergranular carbonate cement precipitated, occupying a large amount of intergranular space and reducing reservoir quality, while also providing sufficient material basis for later dissolution (Figure 14a). Under influence of the Huagang movement, as faults penetrate the reservoir, some aluminum silicate minerals in the feldspar/lithic fragments undergo dissolution, forming grain dissolution pores and a small amount of authigenic kaolinite, quartz, and other dissolution products (Figure 14b). Controlled by the Longjing Movement during the period of structural inversion, intensified fault activity led to the infiltration of acidic atmospheric water along the faults into the sandstone. This results in significant dissolution of the carbonate cement which occupied intergranular volume in the early stage, forming carbonate dissolution pores. Consequently, the reservoir properties are significantly improved, leading to the formation of a reservoir dominated by carbonate dissolution pores and grain dissolution pores as the primary storage space type (Figure 14c).

5.3.2. Carbonate Dissolution Pore Type

In addition to the reservoir characterized by carbonate dissolution pores + grain dissolution pores type, the Upper Huagang Formation of the Yuquan structure also develops reservoirs primarily dominated by carbonate dissolution pore type alone (Figure 14b). During the early stage of clastic particle deposition, a large amount of intergranular carbonate cement precipitates, occupying the interstitial volume and leading to deterioration in reservoir properties (Figure 14a). Due to the differences in fault cutting across the stratigraphic layers, deep hydrocarbon source acidic fluids failed to migrate into the sandstone reservoirs, resulting in no dissolution of aluminum silicate particles such as feldspar. Affected solely by the Longjing movement, acidic atmospheric water infiltrated along the faults into the sandstone reservoirs of the Upper Huagang Formation, causing significant dissolution of carbonate cement. This resulted in the formation of a reservoir dominated by carbonate dissolution pores (Figure 14c).

5.3.3. Particle Dissolution Pore Type

During the early stage of clastic particle deposition, in an alkaline fluid environment, intergranular carbonate cement and chlorite of particle edge precipitated. The former occupies a certain intergranular volume, providing a material basis for later-stage dissolution, while the latter effectively inhibits the cement block in the intergranular throat, providing a pathway for the entry of dissolution fluids (Figure 14a). Subsequently, under the influence of the Huagang movement, acidic hydrocarbon fluids from the Pinghu Formation infiltrated along the faults into the reservoir, causing dissolution of aluminum silicate particles

such as feldspar/lithic fragments to form particle dissolution pores (Figure 14b). Under the intense influence of the Longjing movement, fractures experienced significant activity, leading to the infiltration of acidic hydrocarbon fluids and acidic atmospheric water into the reservoir. The dissolution of aluminum silicate particles such as feldspar/lithic fragments was further enhanced, resulting in significant improvement in reservoir quality. Additionally, some carbonate cement also underwent dissolution, forming a small number of carbonate dissolution pores (Figure 14c). The Lower Huagang Formation mainly develops reservoirs dominated by particle dissolution pores.

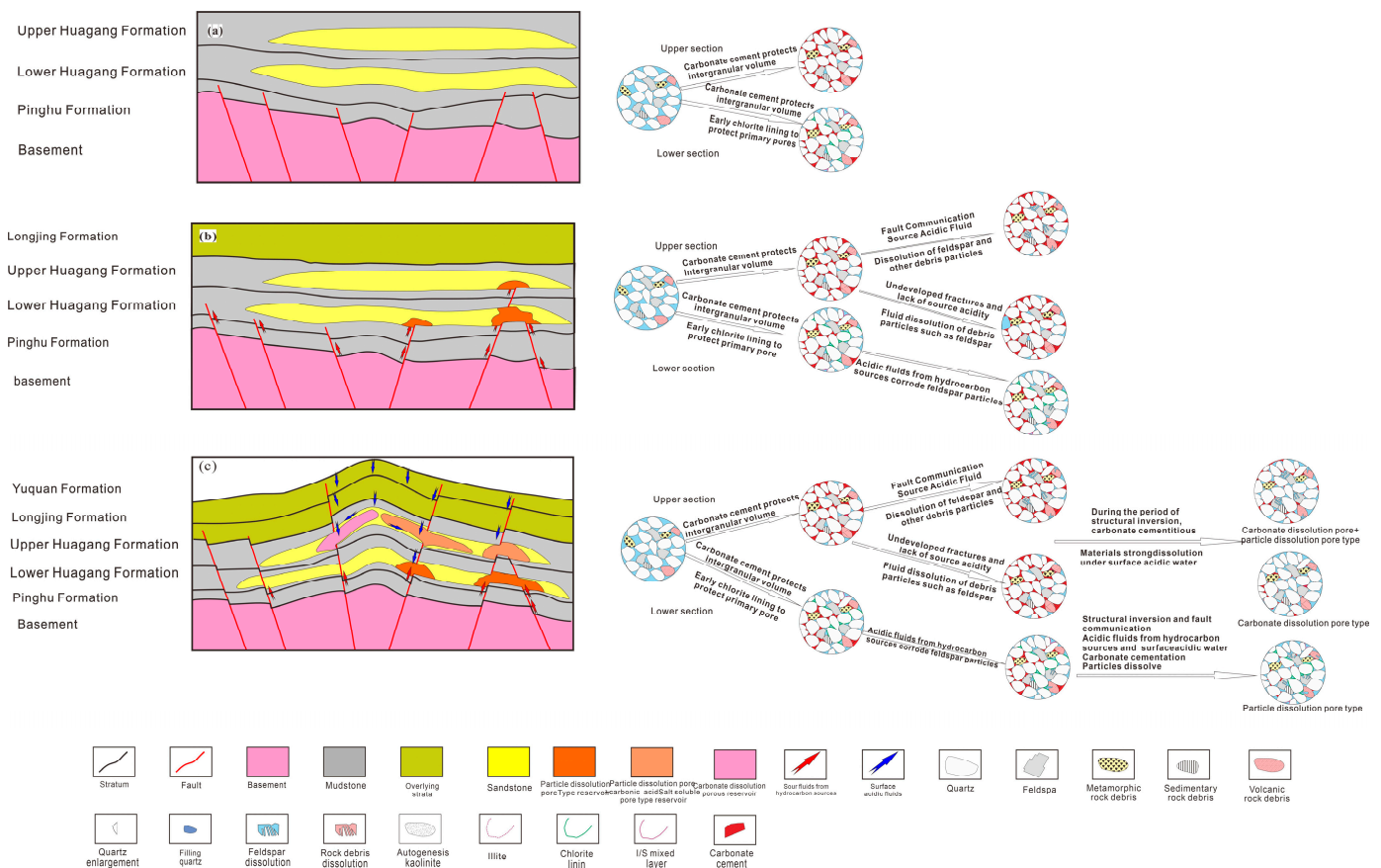


Figure 14. Development model diagram of the Huagang Formation of the Yuquan Structure. (a) Depositional early stage of the Huagang Formation. (b) Huagang Movement period. (c) Longjing Movement period.

6. Conclusions

The majority of sandstones in the Huagang Formation of the Yuquan structure have a latest diagenetic stage of intermediate diagenesis stage A, and some sandstones have a latest diagenetic stage of intermediate diagenesis stage B. Different authigenic minerals and the same authigenic mineral at different stages reduce storage space. Compaction and strong tectonic compression are the main reasons for pore damage.

The pore spaces in the sandstone reservoirs of the Yuquan Huagang Formation are mainly composed of dissolution pores, with very few residual intergranular pores. Three main types of reservoirs are developed, and the carbonate dissolution pores + grain dissolution pores type and carbonate dissolution pore type are the main reservoir types in the Upper Huagang Formation. The grain dissolution pore type is the reservoir type in the Lower Huagang Formation.

In the sandstone of the Upper Huagang Formation of the Yuquan structure, the role of carbonate exhibits a typical preservational diagenetic effect during the pore evolution process. This effect involves occupying the interstitial volume during early burial, resisting

structural compression's damage to the interstitial volume, resulting in dense sandstone of the upper sub-segment at shallow burial depths. However, after the structural inversion movements, these early precipitated carbonates undergo intense dissolution under the action of atmospheric water, thereby improving sandstone's properties and forming reservoirs.

The structural features during the inversion period and the configuration relationship with the sandstone are the determinants of reservoir formation. During the tectonic uplift, faults connected atmospheric water with the Huagang Formation sandstone, leading to the strong dissolution of sandstone. In particular, the dissolution of carbonates leads to the formation of reservoirs with good pore properties.

Author Contributions: Conceptualization, Z.L. (Zhengxiang Lv); data curation, B.C.; funding acquisition, C.X. and Z.L. (Zhengxiang Lv); investigation, C.X. and Z.L. (Zhengxiang Lv); formal analysis, C.X. and B.X.; methodology, Y.Q.; project administration, Z.L. (Zheyuan Liao); resources, Y.Q., B.X. and Z.L. (Zheyuan Liao); supervision, Y.C.; validation, Z.L. (Zhengxiang Lv); visualization, Y.Q.; writing—original draft, Y.Q.; writing—review and editing, Y.C., C.X. and Z.L. (Zhengxiang Lv). All authors have read and agreed to the published version of the manuscript.

Funding: (1) Research on deep/ultra-deep hydrocarbon formation conditions and mechanism in Back-arc basin—West Lake Sag (Projects of China grant number KJGG2022-0402). (2) Origin, Vulnerability, and Ecological Protection of Geological Relics in the Upstream of Dadu River (Grant No. 2022YFS0488), Supported by Sichuan Science and Technology Program.

Data Availability Statement: Data are contained within the article.

Acknowledgments: We appreciate the constructive suggestions received from Yonghuang, Cai. We also thank the CNOOC (China) Limited Shanghai Branch for data support.

Conflicts of Interest: The authors declare no conflicts of interest.

References

1. Xiao, H.; Wang, H.N.; Yang, Y.D.; She, H.Q. Influence of diagenetic evolution on tight sandstone reservoir flow capacity. *Pet. Geol. Exp.* **2019**, *41*, 800–811.
2. Tian, B.; Zheng, Y.; Zhao, J.; Zhu, X.; He, T.; Luo, X. Research Development in Anomously High Porosity of Deep Clastic Reservoirs. *Sci. Technol. Eng.* **2022**, *22*, 9456–9465. (In Chinese)
3. Liu, Z.; Li, S.; Zhang, J.; Li, W.; Li, M.; Xu, Q. Quantitative Study of Diagenesis and Dissolution Porosity in Conglomerate Reservoirs. *Chem. Technol. Fuels Oils* **2023**, *58*, 1035–1045. [[CrossRef](#)]
4. Shen, Y. A Study on the Sedimentary Facies of the Huagang Formation in the West Lake Sag. Master's thesis, China University of Petroleum, Dongying, China, 2018. (In Chinese). [[CrossRef](#)]
5. Zhou, X. Geological understanding and innovation in Xihu sag and breakthroughs in oil and gas exploration. *China Offshore Oil Gas* **2020**, *32*, 1–12.
6. Yuan, G. Dissolution Mechanism of Feldspar and Carbonate Minerals During Rock-Forming Process and Its Physical Response. Ph.D. thesis, China University of Petroleum, Dongying, China, 2014. (In Chinese).
7. Huang, X.; Lin, C.Y.; Huang, D.W.; Duan, D.; Lin, J.; He, X.; Liu, B. Diagenetic differential evolution of Huagang Formation sandstone reservoir in the north-central part of central reversal structural belt in Xihu Sag. *Pet. Geol. Recovery Effic.* **2022**, *29*, 1–14.
8. Morgan, C.D.; Bereskin, S.R. Characterization of petroleum reservoirs in the Eocene Green River Formation, Central Uinta Basin, Utah. *Mt. Geol.* **2003**, *40*, 111–127.
9. Schlunegger, F.; Kissling, E. Slab Load Controls Beneath the Alps on the Source-to-Sink Sedimentary Pathways in the Molasse Basin. *Geosciences* **2022**, *12*, 226. [[CrossRef](#)]
10. Lin, T.; Hu, M.; Cai, Q. Characteristics of sedimentary phases of Quan Si section in Wangjiatun area, northern Songliao Basin. *J. Oil Gas* **2013**, *35*, 12–17.
11. Yang, J.; Yang, X.; Zhou, J.; Gan, J.; Song, A.; Jiang, F.; Yang, L. Developmental characteristics and hydrocarbon geological significance of the inversion tectonic zone of the Songnan-Baodao depression in the deep-water area of the Qiongdongdong Basin. *J. Oceanogr.* **2019**, *41*, 97–106, (In Chinese with English Abstract).
12. Zhou, P.; Sun, P.; Liu, C.; Xiong, Z. Study on the spatial and temporal matching relationship between oil and gas formation and storage in the Yuquan tectonics of the Xihu Depression. *Mar. Quat. Geol.* **2024**, *44*, 121–129.
13. Yang, Z.; Huang, Z.; Qu, T.; Li, Z.; Wang, R.; Zhang, J.; Ma, C.; Pan, Y.; Yu, J. Main controlling factors and formation mode of oil and gas in Huangyan area, Xihu Depression, East China Sea Basin. *Geol. Rev.* **2023**, *69*, 2179–2194.

14. Twiss, R.J.; Moores, E.M. *Structural Geology*; Palgrave Macmillan: New York, NY, USA, 2007.
15. Xu, F.; Xu, G.; Liu, Y.; Zhang, W.; Cui, H.; Wang, Y. Factors controlling the development of tight sandstone reservoirs in the Huagang Formation of the central inverted structural belt in Xihu sag, East China Sea Basin. *Pet. Explor. Dev.* **2020**, *47*, 101–113. [[CrossRef](#)]
16. Xu, G.; Cui, H.; Liu, Y.; Wang, Y.; Huang, S.; Zhang, W.; Li, P.; Zhou, P. Relationship between sandstone reservoirs densification and hydrocarbon charging in the Paleogene Huagang Formation of West Lake Sag, East China Sea Basin. *Bull. Geol. Sci. Technol.* **2020**, *39*, 20–29.
17. Zhong, T.; Zhang, W.; Miao, Q. Characteristics and genesis of anomalously high porosity zones in the Huagang Formation sandstones in Xihu sag, East China Sea. *J. Chengdu Univ. Technol.* **2018**, *45*, 478–486.
18. Zhang, Y.Z.; Z, W.; Chen, Z.Y.; Diao, H. Mechanism and geologic significance of “sinking before gathering” of gas reservoirs in the Paleoproterozoic Huagang Formation in the central inversion tectonic zone of the Xihu Depression, East China Sea Shelf Basin. *J. Oil Gas Geol.* **2023**, *44*, 1256–1269.
19. Zhou, X.; Jiang, Y.; Tang, X. Tectonic setting, prototype basin evolution and exploration enlightenment of Xihu sag in East China Sea basin. *China Offshore Oil Gas* **2019**, *31*, 1–10.
20. Yu, Z.-K.; Ding, F.; Zhao, H. Characteristics of structural evolution and classification of hydrocarbon migration and accumulation units in Xihu Sag, China. *Shanghai Land Resour.* **2018**, *39*, 75–78.
21. Zhang, G.; Zhang, J. Characterization of tectonic inversion in the East China Sea shelf basin and exploration of the genesis mechanism. *Geol.Front.* **2015**, *22*, 11.
22. Zhou, R.; Fu, H.; Xu, G.; Miao, Q. Sedimentary stratigraphy of Pinghu Formation-Huagang Formation, Xihu Depression, East China Sea shelf basin. *J. Sedimentol.* **2018**, *36*, 132–141.
23. Jiang, Y.; Zou, W.; Liu, J.; Tang, X.; He, X. Tectonic genesis of the late Miocene reversed backslope in the Xihu Depression, East China Sea: New insights from basal structural differences. *Earth Sci.* **2020**, *45*, 968–979.
24. Wang, L. The Tectonic Evolution of the Yuquan Structure and Its Surrounding Areas in the East China Sea. Master’s thesis, Ocean University of China, Qingdao, China, 2010. (In Chinese)
25. Guo, Z.; Liu, C.; Tian, J. Structural characteristics and main controlling factors of inversion structures in West Lake Sag in Donghai Basin. *Earth Sci. Front.* **2015**, *22*, 59–67.
26. Dong, C.M.; Zhao, Z.X.; Zhang, X.G.; Yu, S.; Huang, X.; Duan, D.P.; Lin, J.L.; Sun, X.L. Analysis of provenance and sedimentary facies of Huagang formation in the north-central of Xihu sag. *J. Northeast Pet. Univ.* **2018**, *42*, 25–34.
27. Zhang, G.; Liu, J.; Qin, L.; Zhao, H. Characteristics of the large braided river depositional system of the Oligocene Huagang Formation in the Xihu sag. *China Offshore Oil Gas* **2018**, *30*, 10–18.
28. Xu, F. Reservoir Characteristics and Controlling Factors of the Paleocene Huagang Formation in the Central Inversion Tectonic Zone of the Xihu Depression. Master’s thesis, Chengdu University of Technology, Chengdu, China, 2017. (In Chinese).
29. Gao, Y.; Fu, H.; Zhao, L.; Ge, H.; Fu, Z. Stratigraphic sequence of the Huagang Formation, Xihu Depression, East China Sea. *Sediment. Tethys Geol.* **2014**, *34*, 24–29. (In Chinese with English Abstract).
30. GB/T29172-2012; Practices for Core Analysis. Standardization Administration of China: Beijing, China, 2012.
31. SY/T 5163-2010; National Energy Administration. Analysis Method for Clay Minerals and Ordinary Non-Clay Minerals in Sedimentary Rocks by the X-ray Diffraction. Petroleum Industry Press: Beijing, China, 2010.
32. GB/T 14506.28-2010; General Administration of Quality Supervision, Inspection and Quarantine of the People’s Republic of China, Standardization Administration of the People’s Republic of China. Methods for Chemical Analysis of Silicate Rocks—Part 28. Determination of 16 major and minor elements content. Standards Press of China: Beijing, China, 2011.
33. GB/T 14506.30-2010; General Administration of Quality Supervision, Inspection and Quarantine of the People’s Republic of China, Standardization Administration of the People’s Republic of China. Methods for Chemical Analysis of Silicate Rocks—Part 30. Determination of 44 elements. Standards Press of China: Beijing, China, 2011.
34. SY/T 6010-2011; National Energy Administration. Test Method for Fluid Inclusion in Sedimentary Basins by Microthermometry. Petroleum Industry Press: Beijing, China, 2011.
35. SY/T 5238-2008; National Development and Reform Commission. Analysis Method for Carbon and Oxygen Isotope of Organic Matter and Carbonate. Petroleum Industry Press: Beijing, China, 2008.
36. SY/T6285-2011; Petroleum Geological Exploration Professional Standardization Committee. Oil and Gas Reservoir Evaluation Method. National Energy Administration: Beijing, China, 2011.
37. Lei, C.; Ye, J.R.; Wu, J.F.; Shan, C.; Yin, S. Dynamic Process of Hydrocarbon Accumulation in Low-Exploration Basins: A Case Study of West Lake Sag. *EarthSci. J. China Univ. Geosci.* **2014**, *39*, 837–847.
38. Keith, M.L.; Weber, J.N. Carbon and oxygen isotopic composition of selected limestones and fossils. *Geochim. Et Cosmochim. Acta* **1964**, *28*, 1787–1816. [[CrossRef](#)]
39. Yin, G.; Ni, S. *Isotope Geochemistry*; Geological Publishing House: Beijing, China, 2009.

40. Friedman, I.; O'Neil, J.R. Compilation of stable isotope fractionation factors of geochemical interest. In *Data of Geochemistry*, 6th ed.; Professional Paper; United States Government Printing Office: Washington, DC, USA, 1977; pp. 1–12.
41. SY/T 5477-2003; Classification of the Stages of Petrogenesis of Clastic Rocks. State Economic and Trade Commission: Beijing, China, 2003.
42. Huang, S.; Huang, P.; Wang, Q.; Liu, H.; Wu, M.; Zou, M. The significance of cementation in porosity preservation in deep-buried sandstones. *Lithol. Reserv.* **2007**, *3*, 7–13.

Disclaimer/Publisher's Note: The statements, opinions and data contained in all publications are solely those of the individual author(s) and contributor(s) and not of MDPI and/or the editor(s). MDPI and/or the editor(s) disclaim responsibility for any injury to people or property resulting from any ideas, methods, instructions or products referred to in the content.